# Urban modification of heavy rainfall: a model case study for Bhubaneswar urban region

Madhusmita Swain[1,2], Raghu Nadimpalli[1,3,4*] , Ananda K. Das[3], U. C. Mohanty[1] and Dev Niyogi[2,5]

## Abstract

An increase in urbanization has been witnessed from 1980 to 2019 in Bhubaneswar, Odisha. The impact of this increase in urban areas on rainfall pattern and intensity has been assessed in this study. To evaluate these changes, four heavy rainfall events, such as 06th March 2017, 23rd May 2018, 20 – 22 July 2018, and 04 – 08 August 2018, have been simulated with 1980, 2000, and 2019 land use land cover (LULC) obtained from United States Geological Survey imageries. With these two LULC sensitivities, urban canopy model (UCM) experiments have also been carried out. These experiments suggest that incorporating corrected LULC is necessary for simulating heavy rainfall events using the Weather Research and Forecasting (WRF) model. Urbanization increases the rainfall intensity, and the spatial shift was more pronounced along the peripheral region of the city. The vertically integrated moisture flux analysis suggests that more moisture present over the area received intense rainfall. An increase in urbanization increases the temperature at the lower level of the atmosphere, which increases [planetary boundary layer height, local convection, and rainfall over the region. Contiguous Rain Area method analysis suggests that the 2019 LULC with single layer UCM predicts a better spatial representation of rainfall. This combination works well for all the four cases simulated.

## Highlights

• Realistic representation of Land Use and Land Cover (LULC) changes improves the prediction of convection over urban regimes.

• The 2019 urban amalgamation in LULC spread in the weather model discloses that the rainfall intensity has increased compared to the 1980 LULC simulation

• The maximum rainfall limited to a shorter spell (~1 hour), due to the urban heating effect.

**Keywords** Urban area, Heavy Rainfall, UCM, WRF model, Bhubaneswar

*Correspondence:
Raghu Nadimpalli
raghu.met2012@gmail.com
[1] School of Earth, Ocean and Climate Sciences, Indian Institute
of Technology Bhubaneswar, Odisha 752050, India
[2] Department of Agronomy, and Department of Earth, Atmospheric,
and Planetary Sciences, Purdue University, West Lafayette, IN 47907, USA
[3] India Meteorological Department, Delhi, India
[4] Scientist – C, Urban Meteorology and Climate Cell, India Meteorological
Department, New Delhi, India
[5] Department of Geological Sciences, Jackson School of Geosciences,
and Department of Civil, Environmental and Architectural Engineering,
The University of Texas at Austin, Austin, TX 78712, USA

# 1 Introduction

Urbanization is the land use land cover (LULC) changes of the region, which creates contrasts between urban and rural areas land surface characteristics. In recent years, there is an increase in number of extreme rainfall events over different cities of India (Niyogi et al., 2018). Urbanization changes the rainfall distribution; which changes water cycle of the region. Hence, research on urban impacts on rainfall has become more critical in recent periods.

Different studies on urbanization suggest that unchecked urbanization can promote floods in a region (Ghosh et al., 2012; Gupta & Nair, 2010; Kishtawal et al., 2010). Urban land cover modulates local weather and climate processes (Yan et al., 2016). LULC changes could modify the emissivity, roughness, humidity, of surface and CAPE values of the atmosphere (Osuri et al., 2017; Pielke et al., 2011). An increase in urbanization can affect the timing and location of rainfall (Lin et al., 2008; Niyogi et al., 2020). Urban land surface alters heat, momentum, and moisture between the atmosphere and surface (Oke, 1988; Shepherd, 2013). Urban heat island (UHI) within the urban region influence dynamical and convective processes in the atmosphere. Natural landscape over urban areas changes rainfall, mesoscale convection, and temperature (Niyogi et al., 2006, 2011). Over city region, higher surface temperature and deeper atmospheric boundary layer are generally observed (Rozoff et al., 2003). The tendency for thunderstorm formation is moreover large cities compared to rural areas (Horton, 1921; Shepherd, 2005).

During the summer months, the Metropolitan Meteorological Experiment suggests that the precipitation over an urban area generally increases (Changnon et al., 1977 and Huff, 1986). From Huff & Vogel, 1978, & Changnon et al., 1991, it is found that the increased rainfall is typically observed within 50 – 75 km downwind of the urbanized city. Due to urbanization, afternoon thunderstorms increased by 67% in Taipei (Chen et al., 2007). Shephard et al. 2002 and Balling & Cerveny, 1987 have noted that the urban heat-island significantly impacts precipitation.

The main objective of this recent work is to find out the role of urbanization on spatial and temporal distribution of heavy rainfall with the help of a mesoscale model over Bhubaneswar, the capital city of Odisha state. An increase in an urban area and its impact on the temperature in Bhubaneswar city has been studied by Pathy and Panda (2012), Swain et al. (2017), Gogoi et al. (2019), and Barik et al. (2019). In this study, we want to address how the evolution of urban areas changes the intensity and characteristics of rainfall over a region? Four heavy rainfall events have been considered, and the Weather Research and Forecasting (WRF) model is used to simulate those cases. These simulations are conducted by incorporating images of land-surface characteristics of the Bhubaneswar urban area for heavy rainfall events.

# 2 Study area

Bhubaneswar is an ancient city with a population of 8.38 lakhs located along the eastern portion of India. It is centered at 85.84º E and 20.27º N, 45 m from the mean sea level. This is situated in the Khordha district of Odisha state. It is surrounded by Nayagarh district on the west, Cuttack district on its north, Puri district on its south, and Jagatsinghpur district on the east. Bhubaneswar is one of the urbanized cities in the country, which experiences frequent natural hazards such as heatwaves, heavy rainfall, and tropical cyclones (Gupta, 2020; Mohanty et al., 2013; Panda et al., 2014).

# 3 Model configuration

In the research work, the Advanced Research version of the Weather Research and Forecast model (WRF-ARW) has been used (Skamarock et al., 2008) to simulate the heavy rainfall events. The model consists of a three-domain, in which third domain consists of 500 m grid spacing (d03), a second domain consists of 1.5 km grid spacing (d02), and an outer domain consists of 4.5 km grid spacing (d01). The domain used for rainfall events model simulation has been shown in Fig. 1a and the satellite view of d03, consisting of Bhubaneswar and Cuttack urbanized city presented in Fig. 1b.

# 4 Data used and methodology

To analyze the effect of urbanization on rainfall, four heavy rainfall events have been considered, such as 06th March 2017 (72 mm/hr), 23rd May 2018 (55 mm/hr), 20 – 22 July 2018 (220 mm/day), and 04 – 08 August 2018 (390 mm/day). Rainfall analysis for all four cases have been shown in this manuscript. As the rainfall prediction is better for 20,072,018 case, all other large-scale meteorological parameters have been analyzed for this one case only. National Centers for Environmental Prediction (NCEP) Global Forecast System (GFS) analysis of $0.5° \times 0.5°$ spatial resolution datasets have been used to run the model. For validation, half-hourly rainfall data of $10\,km \times 10\,km$ grid resolution from Global Precipitation Measurement (GPM) have been used. GPM from NASA is the best reliable datasets during the study period and over the study region. However, in recent years from last few months, the surface network density has been increased over the Odisha State Disaster Management, unfortunately which is not available during the study period.
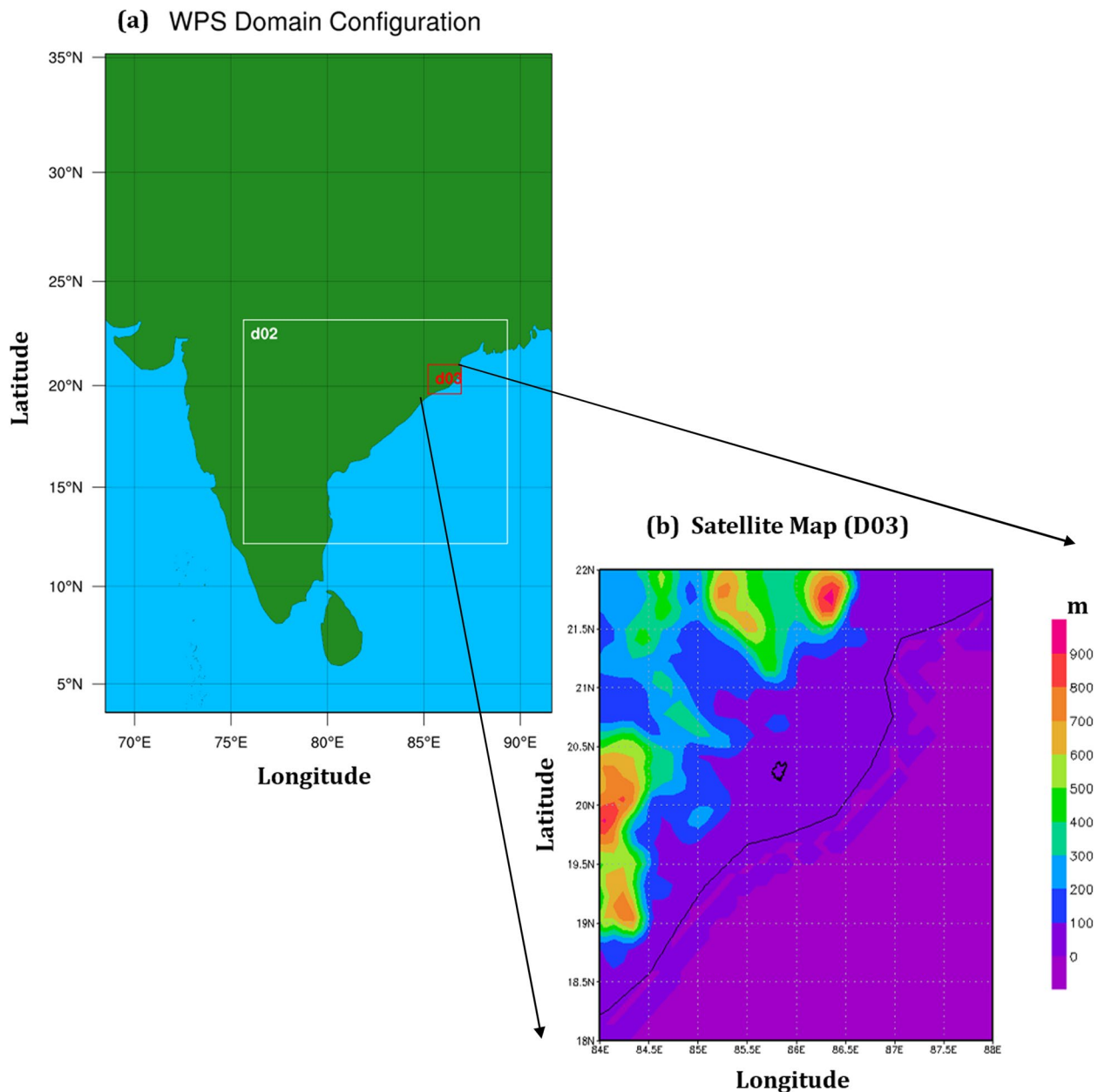
**Fig. 1 a** Model domain considered for the study, and **b** Extension of D03 with elevation height in shaded

Urban Land Use Land Cover (LULC) maps have been incorporated only in the inner domain of the model setup. United States Geological Survey (USGS) imageries have been taken and with the help of ArcGIS software, the land use maps for 1980, 2000, and 2019 year for Bhubaneswar-Cuttack city has been created. A total of seven experiments for each rainfall case have been carried out with different LULC and Urban Canopy Model (UCM) named Control, 1980_NoUCM, 1980_SUCM, 2000_NoUCM, 2000_SUCM, 2019_NoUCM, and 2019

SUCM. Here Control is referred to as simulation with default land use. 1980_NoUCM suggests the model simulation with 1980 LULC without incorporating the UCM layer, whereas 1980_SUCM suggests the model simulation with 1980 LULC and single layer UCM. Similarly, 2000_NoUCM and 2000_SUCM are the same as 1980_NoUCM and 1980_SUCM but with 2000 LULC incorporation, and 2019_NoUCM and 2019_SUCM are the same as 1980_NoUCM and 1980_SUCM but with 2019 LULC incorporation. The physical parameterizations

Swain *et al. Computational Urban Science*          (2023) 3:2

Page 4 of 19

include the Kain-Fritsch scheme for cumulus convection (which has been considered in the parent domain only), the WDM 6-class scheme for microphysics, the RRTMG shortwave and longwave schemes, the Bougeault and Lacarrere (BouLac) planetary boundary, the Monin–Obukhov Similarity scheme for the surface layer, and the unified Noah Land-Surface Model scheme (Table 1). All the used parameterization schemes have been selected on the basis of our own sensitivity experiments for heavy rainfall prediction over Bhubaneswar city (Nadimpalli et al., 2022; (Karrevula, N. R., Nadimpalli, R., Sinha P., Mohanty S., Swain M., Boyaj A., Mohanty U. C. Performance evaluation of WRF model in simulating heavy rainfall events over Bhubaneswar urban region of East coast of India, under review), and Swain et al. MAPEX-2019). Also the physical parameterization schemes have been chosen from Skamarock et al. (2005). All the four cases have been analyzed and the rainfall results also shown in the manuscript. For only one case (20–22 July 2018), all meteorological parameters have been studied, and presented here.

### 4.1 Contiguous Rain Area (CRA)

The Contiguous Rain Area (CRA) is an object-oriented method to compare the characteristics of forecasted rainfall with observation (Ebert & McBride, 2000). A significant advantage of this method is that the location error of the forecasted rainfall can be quantified.

In the CRA method, the total error is divided into location, volume, and pattern error (Ebert & Gallus, 2009). In CRA, first it will create an area with a user-specified rainfall intensity threshold in both observation and the model forecast. After identifying the observation and forecast pair for a threshold, a pattern-matching technique estimates the location error. Then, till the best-fit between forecast and the observations, the forecast rainfall is horizontally shifted

**Table 1** Model configuration

| Model core | WRF ARW v4 |
| --- | --- |
| Horizontal Resolution | D01: 4.5 km (68 – 92˚ E, 3 – 35˚ N) |
| | D02: 1.5 km (76 – 89˚ E, 12 – 23˚ N) |
| | D03: 0.5 km (85.2 – 87˚ E, 19.5 – 21.5˚ N) |
| Radiation | RRTMG scheme for long-wave and short-wave radiation |
| Cumulus scheme | Kain Fristch |
| PBL scheme | Bougeault and Lacarrere (BouLac) scheme |
| Micro physics | WRF Double Moment-6 (WDM-6) |
| Initial and boundary conditions | NCEP GFS (0.5° × 0.5°) |
| Land surface | Unified Noah |
| Surface Layer | Monin–Obukhov Similarity scheme |

over the observational rainfall. The best fit between the observation and model forecast can be analysed either:

- By overlapping the centers of gravity
- By maximizing the correlation coefficient (Grams et al., 2006)
- By minimizing the total squared error (Ebert & McBride, 2000)
- Maximizing the overlap (Ebert et al., 2004) of the two entities

The original forecast's mean squared error (MSE) can be decomposed into three categories, such as displacement, pattern, and volume error.

$$MSE_{Total} = MSE_{Displacement} + MSE_{Volume} \\ + MSE_{Pattern} \tag{1}$$

where the component errors are,

$$MSE_{Displacement} = 2S_f S_o (r_{opt} - r),$$
$$MSE_{Volume} = (F - O),$$
$$MSE_{Pattern} = 2S_f S_o (1 - r_{opt}) + (S_{f-}S_o)^2$$

where,

O and F = observation and mean forecast values after translation of forecast concerning the observation.

$S_o$ and $S_f$ = standard deviation of the observed and forecast rainfall before translation the forecast.

'r' = spatial correlation between the observation and forecast, and $r_{opt}$ is the optimum value of 'r' during pattern matching.

## 5 Results and discussions

The spatial distribution of rainfall from GPM datasets and all model simulations for four rainfall event has been plotted in Figs. 2 and 3a–h.

For 22052018 case, the control experiment does not predict the rainfall over Bhubaneswar at all. 1980 LULC simulations predicts the rainfall, but not over the Bhubaneswar and it is more spatially scattered. Similarly, for 2000 LULC simulations, the rainfall is also not that much present over Bhubaneswar and it is spatially more scattered. In 2019 LULC simulations, the rainfall is well predicted over Bhubaneswar and its surrounding regions, but the patch of maximum rainfall is spatially shifted towards north (Fig. 2).

Similarly, for 06032017 case, the rainfall has not been well predicted in control, and 1980 LULC simulations. 2000 LULC simulations give rainfall patches over Bhubaneswar, but spatially it is shifted compare to the observation. Simulations with 2019 LULC give rainfall along the eastern side of the city as observation, and
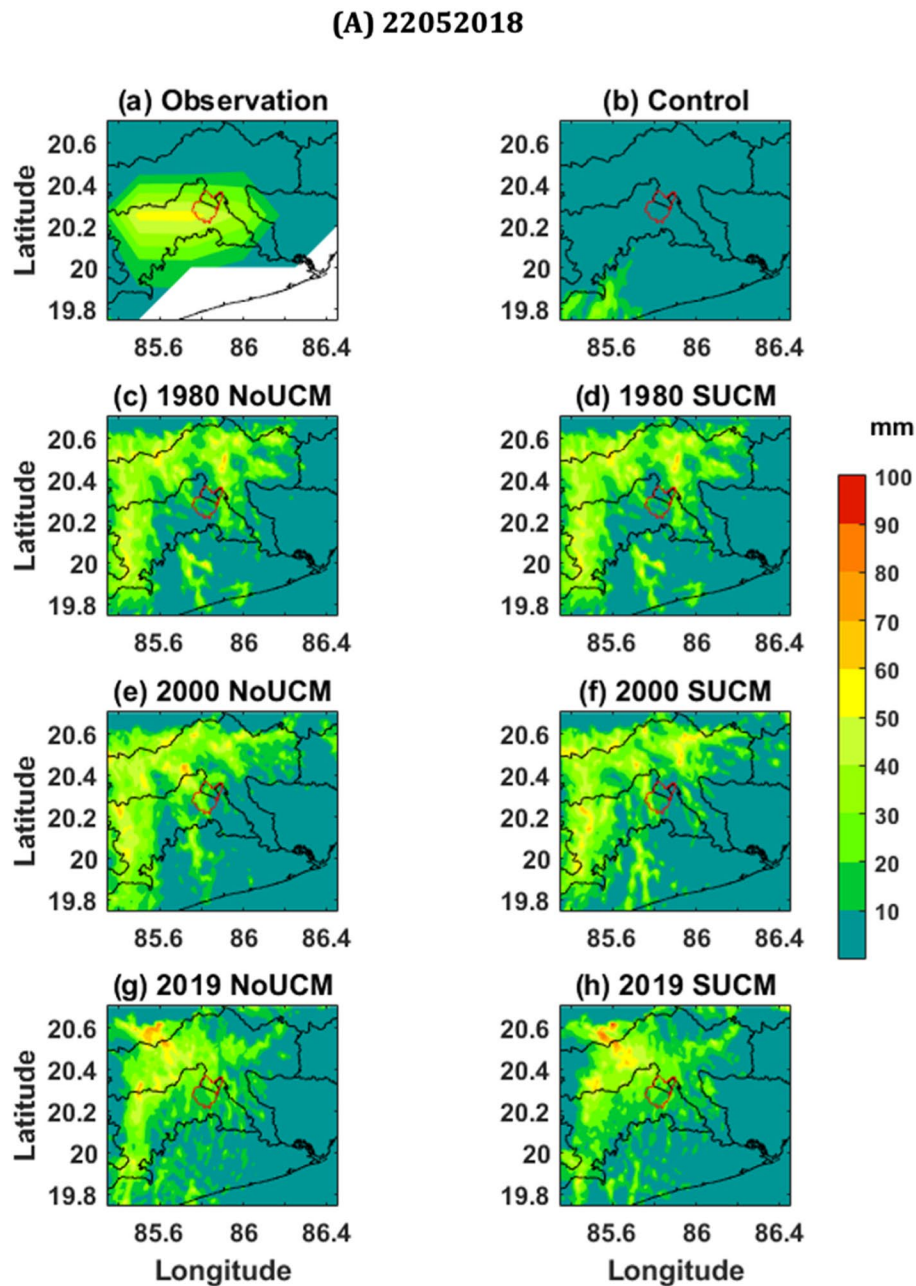
## (A) 22052018



**Fig. 2** Spatial representation of rainfall from for 22052018 case from **a** GPM observation, **b** Control run, **c** 1980 NoUCM, **d** 1980 SUCM, **e** 2019 NoUCM, **f** 2019 SUCM; red color shape file represents Bhubaneswar city

2019_SUCM simulation predicts rainfall intensity better than 2019_NoUCM simulation (Fig. 4).

For 05082018 case, the control, 1980 LULC simulations, and 2000 LULC simulations are predicting rainfall but at the eastern side of the city, whereas the observation gives rainfall along western side of the city. 2019_NoUCM simulation gives rainfall over Bhubaneswar,

but there is a spatial shifting. 2019_SUCM simulation gives two patches of rainfall, one is over Bhubaneswar and another one is along western side of the city near to observed rainfall (Fig. 5).

For 20072018 case, the control, 1980 LULC simulations, and 2000 LULC simulations does not predict rainfall as observation. 2019 LULC simulations predict intensified rainfall as observation, and 2019_SUCM
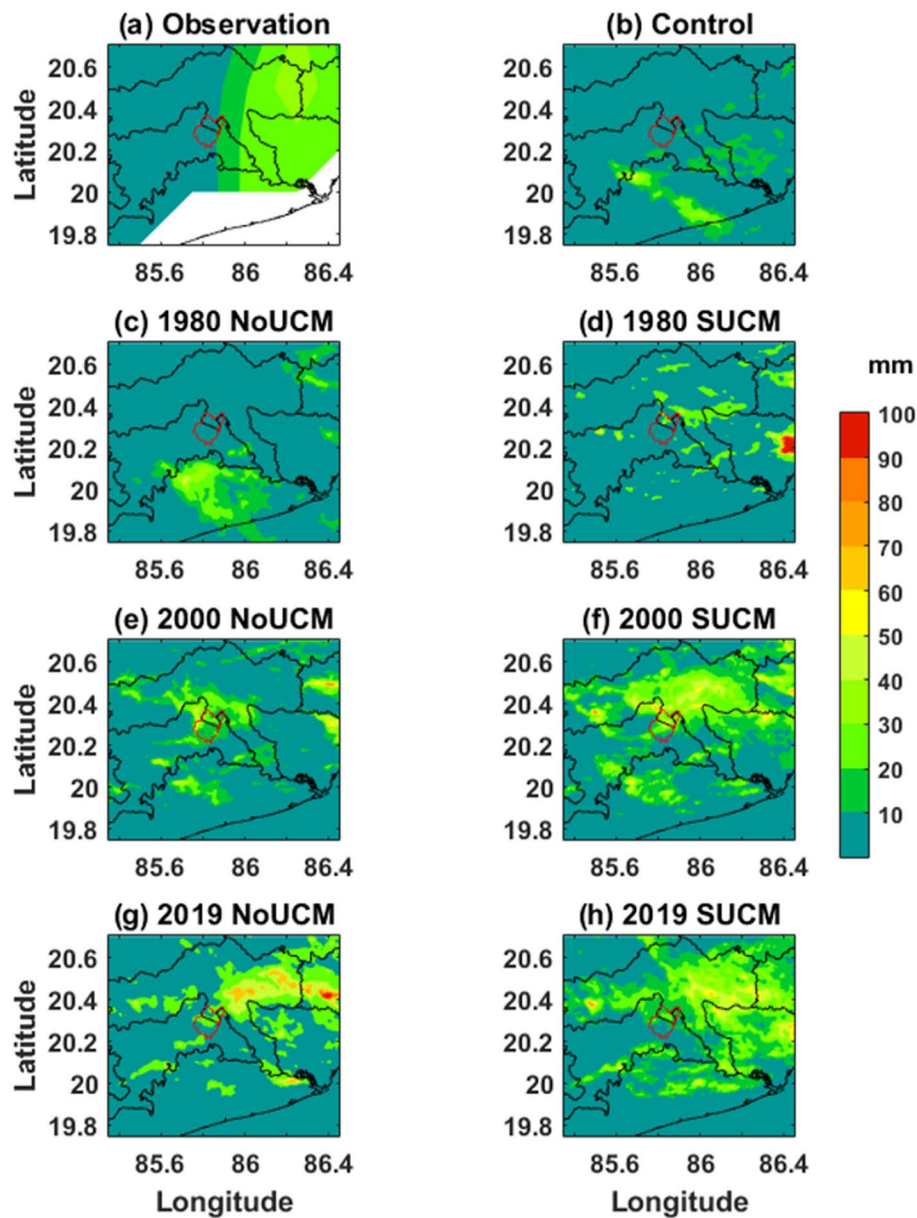
**(B) 06032017**



**Fig. 3** Same as Fig. 2, but for 20072018 case

gives rainfall over eastern side of the city as observation (Fig. 3). Previous studies also observed that the areas with more urban areas are showing a significant increase in extreme precipitation indices in the USA (Mishra and Lettenmaier 2011). It is also observed that the rainfall occurring due to 2019 LULC is present at the periphery of the city, which corroborates with prior observational studies (Zhong & Yang, 2015).

### 5.1 Heidke skill score

Heidke skill score (HSS) is a measure of skill in forecast. It is defined as $=$ (score value – score for the standard forecast) / (perfect score – score for the standard forecast) (Pattanaik et al. 2012).

The range of the HSS is $-\infty$ to 1. Negative values indicate that the chance forecast is better, 0 means no skill, and a perfect forecast obtains a HSS of 1. It measures
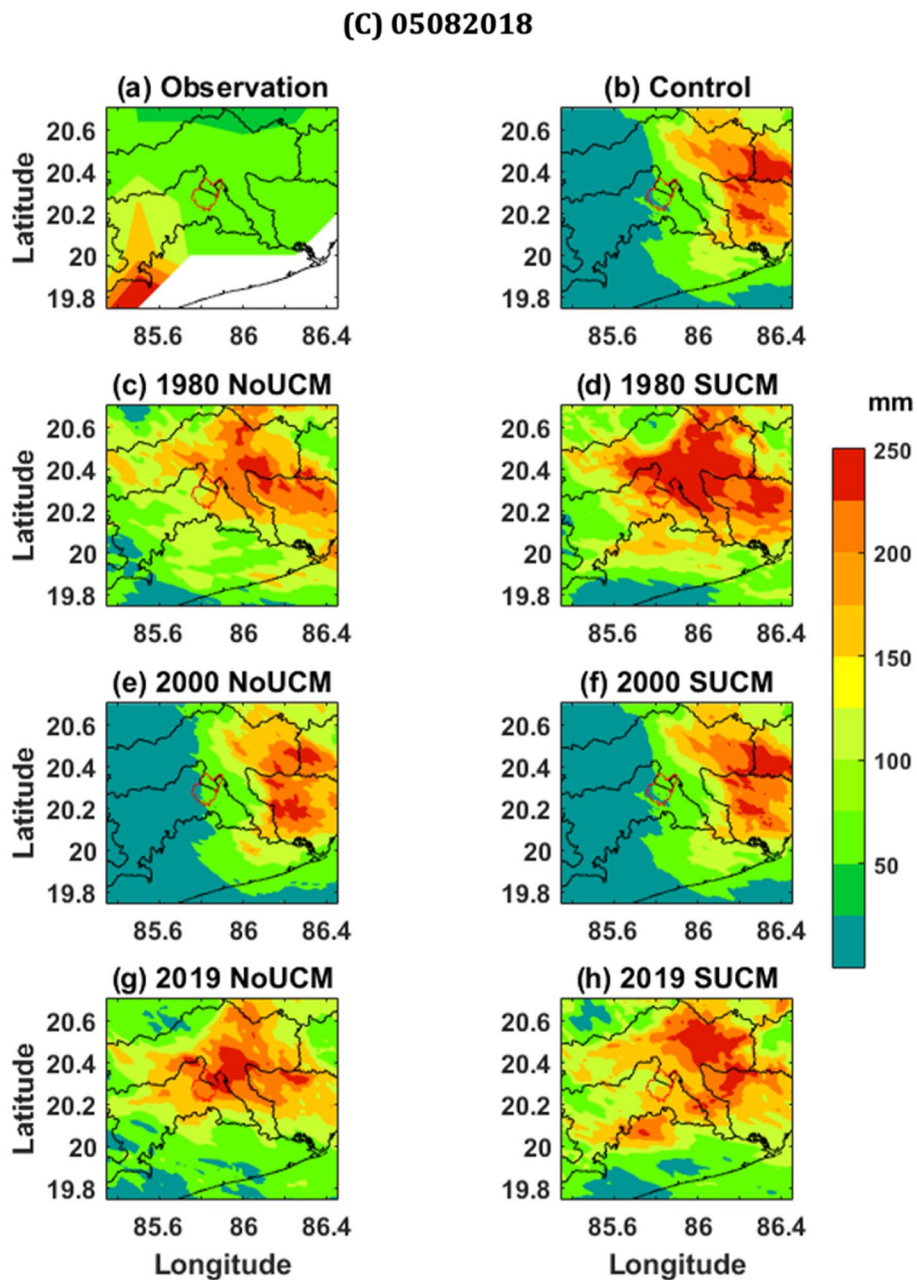
**Fig. 4** Same as Fig. 2, but for 06032017 case

the fractional improvement of the forecast over the observation.

Heidke skill score has been calculated for all the four cases and presented in Fig. 6. It is observed that 2019 LULC simulations are giving good skill score for less intensified rainfall i.e. for 10 – 30 mm for 22052108 case. Similarly, for 06032017 case, 2019 LUC simulations are giving good skill for 0.1 – 20 mm amount of rainfall. As the spatial distribution is not good, the skill score is not coming good for high intensified rainfall. But for 05,082,018 case, it is different like 2000 LULC simulations are giving better result compare to all other simulations. For 20072018 case, 2019 LULC simulations are giving good skill score compared to all other rainfall simulations and it is good for highly intensified rainfall i.e. 40 – 90 mm. To find out the reason for this type of
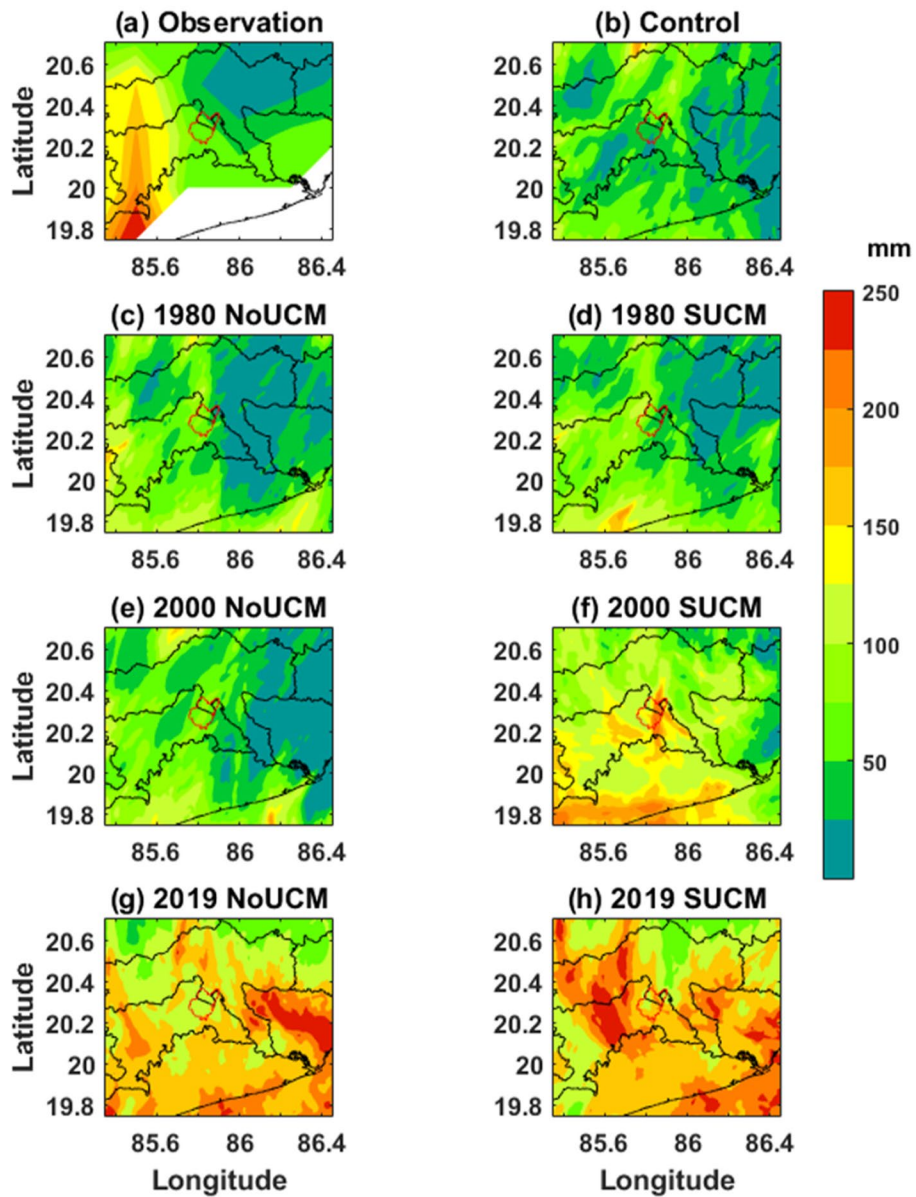
**(D) 20072018**



**Fig. 5** Same as Fig. 2, but for 05082018 case

occurrence, different meteorological parameters have been analyzed and presented in the following section.

### 5.2 Vertically integrated moisture flux

Vertically integrated moisture flux (VIMF) is generally used in meteorology to find out the presence/source of moisture during rainfall. It has been calculated using

following equation from 1000 to 300 hPa vertical pressure level (Banacos & Schultz, 2005),

$$VIMF = -\frac{1}{g} \int_{1000hPA}^{300hPa} \left( \frac{\partial uq}{\partial x} + \frac{\partial vq}{\partial y} \right) dp \qquad (2)$$

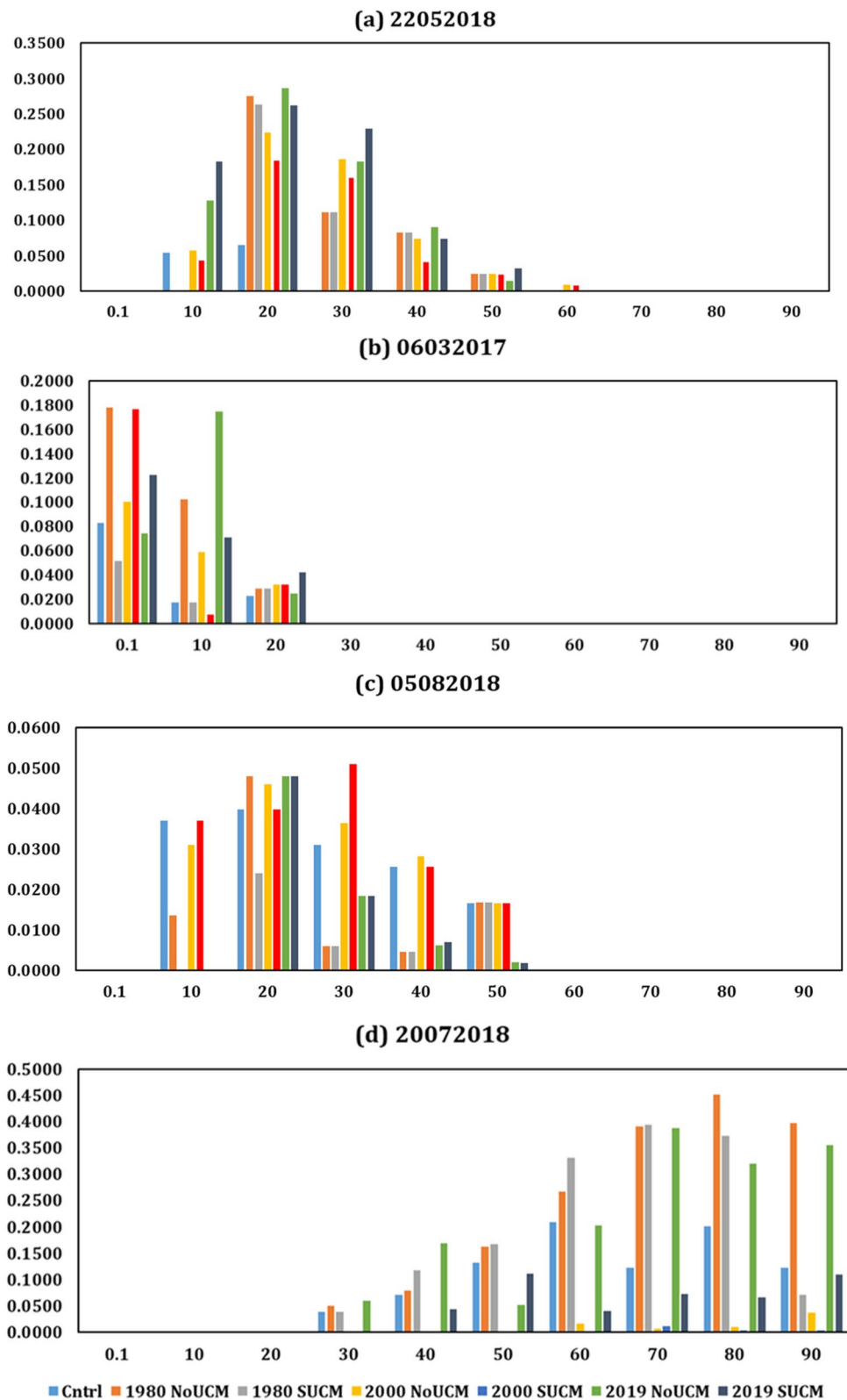In the above equation,
'q' = atmospheric specific humidity,

**Fig. 6** Heidke Skill Score of rainfall of **a** 22052018, **b** 06032017, **c** 05082018 and **d** 20072018 case
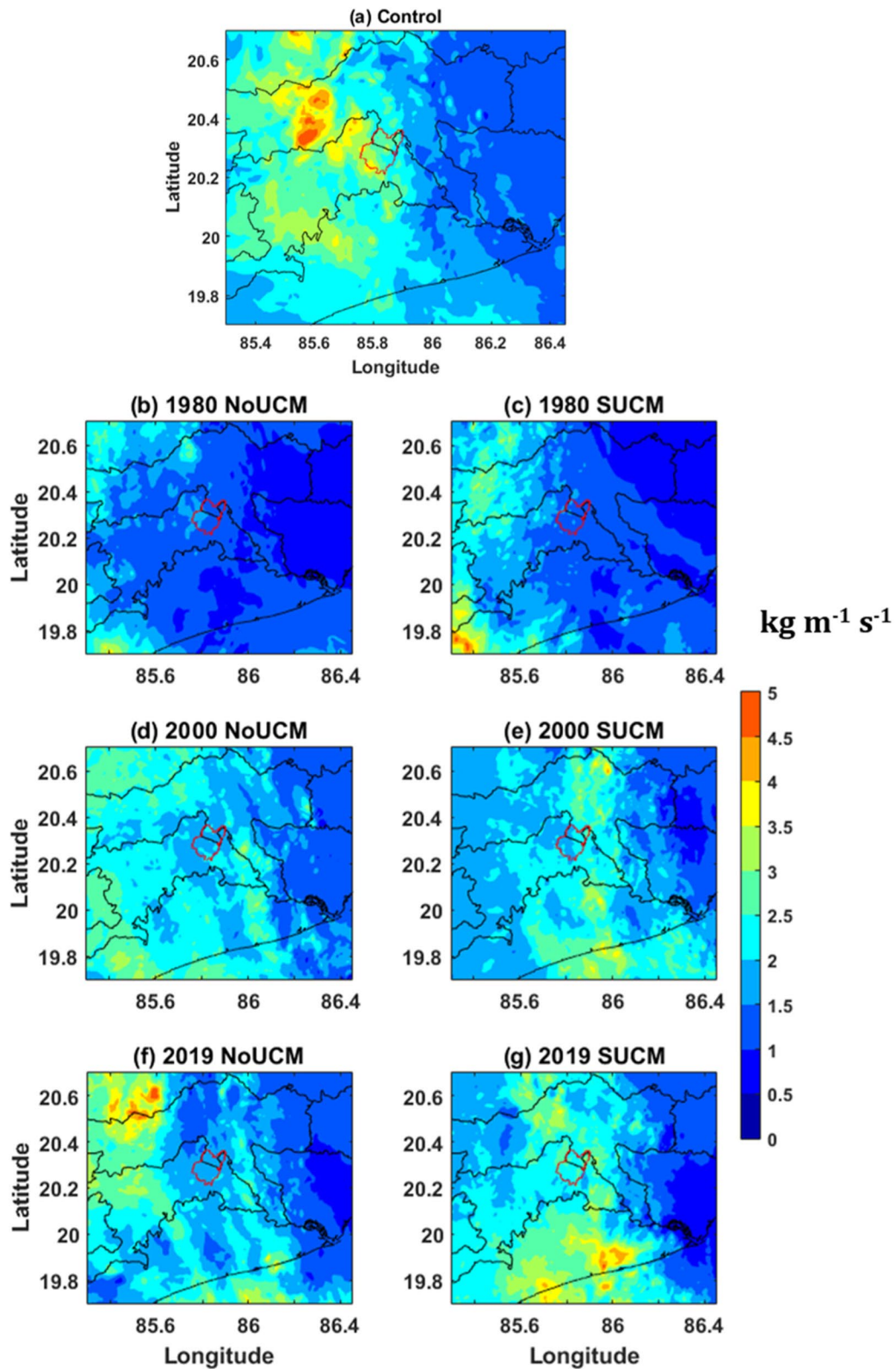
**Fig. 7** Vertically integrated moisture flux (kg m-1 s-1) for 20072018 case **a** control run, **b** 1980 NoUCM, **c** 1980 SUCM, **d** 2000 NoUCM, **e** 2000 SUCM, **f** 2019 NoUCM, and **g** 2019 SUCM

'VIMF' = vertically integrated moisture flux from 1000 to 300 hPa pressure level,

'u' and 'v' = zonal and meridional wind velocity, respectively,

'g' = acceleration due to gravity (= 9.8 m/s2),

and 'p' = atmospheric pressure at different levels (Van Zomeren & Van Delden, 2007).

VIMF for the time of heavy rainfall from all five model simulations has been calculated and shown in Fig. 7a-g. VIMF is generally more for 2019 LULC in both the UCM simulations than 1980 LULC and 2000 LULC, suggesting that the 2019 LUCL predicts a better representation of moisture corresponding to rainfall. Previously, it was also observed that humidity over the urban area is less in comparision to rural areas in many regions of the world, such as Nagano, Japan (Moriwaki et al., 2013), Chicago, USA (Ackerman, 1987), Moscow, Russia (Lokoshchenko, 2017).

### 5.3 Urban energy budget

The surface energy balance is important for thermosdynamical variations above the surface. The urban surface radiation budget and surface energy budget are calculated by using the following equation,

$$Q^* = K\downarrow - K\uparrow + L\downarrow - L\uparrow = Q_H + Q_E \\ + Q_G \dots \left(Wm^{-2}\right) \tag{3}$$

In above equation,

$Q^*$ = net solar radiation at the surface; $K\downarrow$ = incoming shortwave radiation.

$K\uparrow$ = outgoing reflected shortwave radiation and which is defined as $\alpha_0 . K\downarrow$. Where $\alpha_0$ is the surface albedo.

$L\downarrow$ = incoming long-wave radiation on the ground surface.

$L\uparrow$ = outgoing long-wave radiation emitted from the surface, and it is defined as "$\varepsilon_0 \sigma T_s^4 + (1-\varepsilon_0) L\downarrow$". Where, $\varepsilon_0$ = emissivity, Steffan-Boltzmann constant is $5.6704 \times 10^5$ cm$^2$.s$^1$. K.$^4$

$T_s$. = absolute surface temperature.

"$Q_H$" = turbulent sensible heat flux,

"$Q_E$" = turbulent latent heat flux, and.

"$Q_G$" = ground heat flux.

Urban storage from five model simulations has been calculated and presented at constant latitude (20.25° N) with varying longitude and time in Fig. 8a-g. Two vertical black dotted lines represent the geographical spreading of Bhubaneswar city, and the black oval shape represents the temporal occurrence of heavy rainfall over the city. The urban storage is more from the 2019_SUCM simulation and maximum during heavy rainfall. Net radiation over a region represents that the surface absorbs more short-wave radiation. It depends on the geometric and material properties typical of urban areas (Pearlmutter et al., 2005). The increased sensible heat flux results in the region having higher surface air temperature and convection (Zhang et al. 2019).

### 5.4 Vertical velocity

Vertical velocity during heavy rainfall time has been calculated from all model simulations at constant latitude (Bhubaneswar city latitude position: 20.25° N) with varying longitude and vertical pressure level. Then, the vertical velocity from four sensitivity experiments and the control one has been plotted in Fig. 9a-f.

Vertical velocity between 900 to 500 hPa level is more (which is about 4 m s-1) and positive in the 2019_SUCM experiment with respect to the control experiment compared to all other simulations. Positive vertical velocity is associated with rising/ascent mass motion from the surface, while negative vertical velocity is associated with subsidence mass movement towards the surface. The rising mass motion (i.e., moisture) is related to extreme rainfall over a region. It is observed that the urban heat island effect strengthens the vertical velocity along the periphery, which increases the precipitation (Zhang et al., 2018). We can also observe that the rising motion is more around 86° E, a peripheral region of Bhubaneswar. The model with 1980 LULC simulations provides less vertical velocity, suggesting that surface evaporation is less due to less surface air temperature.

### 5.5 Planetary Boundary Layer (PBL) height

As the local convection affects the PBL height of the region, the PBL height has been plotted for the heavy rainfall time over Bhubaneswar city and presented in Fig. 10a-g. It is observed that the PBL height is more in 2019 LULC simulations over Bhubaneswar city compared to 1980 LULC and 2000 LULC simulations. It suggests that the increase in an urban area increases the surface air temperature; which lowers relative humidity and increases PBL height over the city. Over urban areas, an increase in PBL height results in the transfer of more water mixing vapor into the atmosphere (Zhang et al., 2019). Consequently, heavy rainfall events generally occur in urban areas with more localized and pronounced intensity and frequency.

### 5.6 Surface-precipitation feedback

The rainfall over a region is mainly contributed by local evapotranspiration and large-scale atmospheric moisture transport to that region. The antecedent
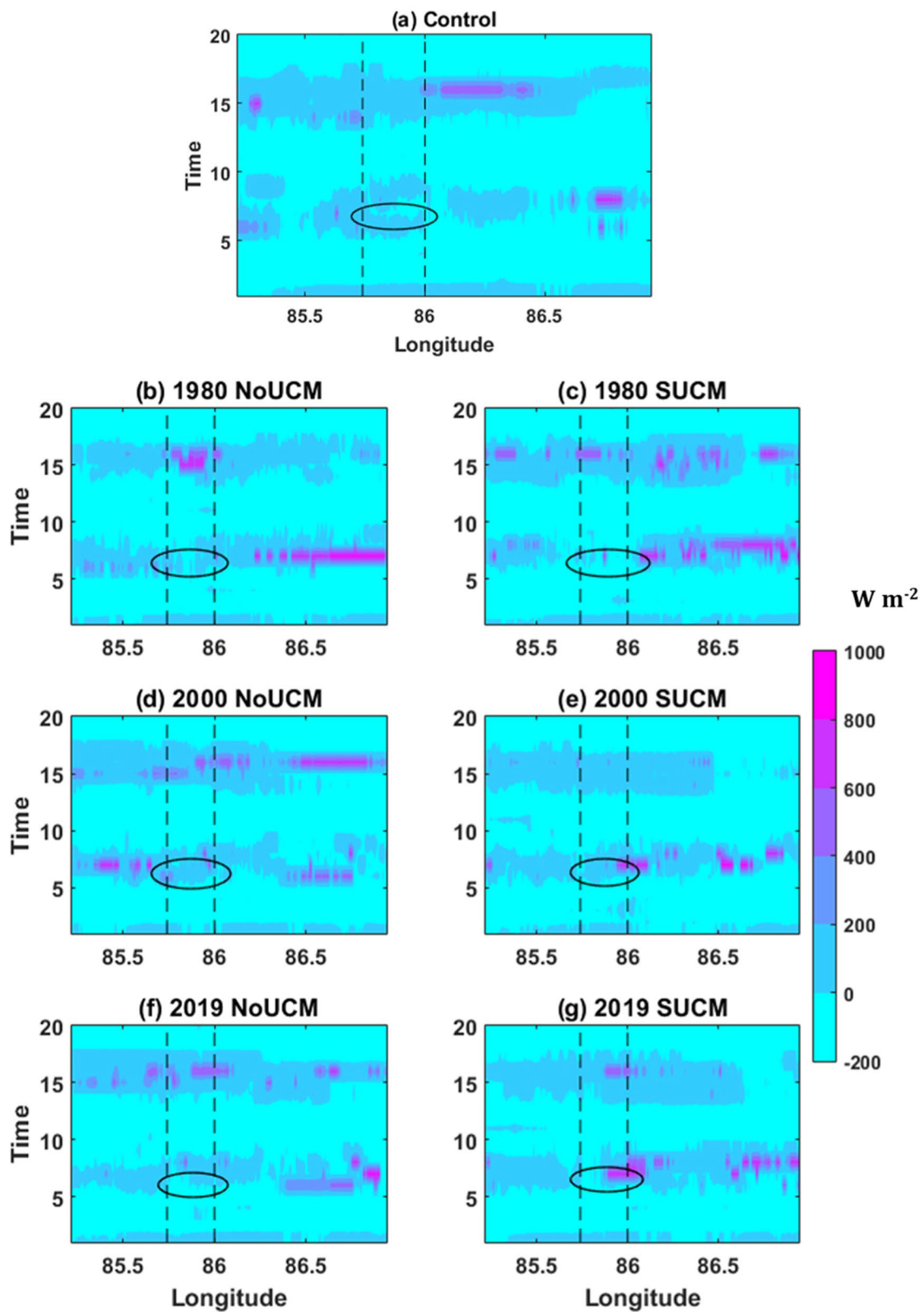
**Fig. 8** Urban storage term (W m-2) for 20072018 case **a** control run, **b** 1980 NoUCM, **c** 1980 SUCM, **d** 2000 NoUCM, **e** 2000 SUCM, **f** 2019 NoUCM, and **g** 2019 SUCM
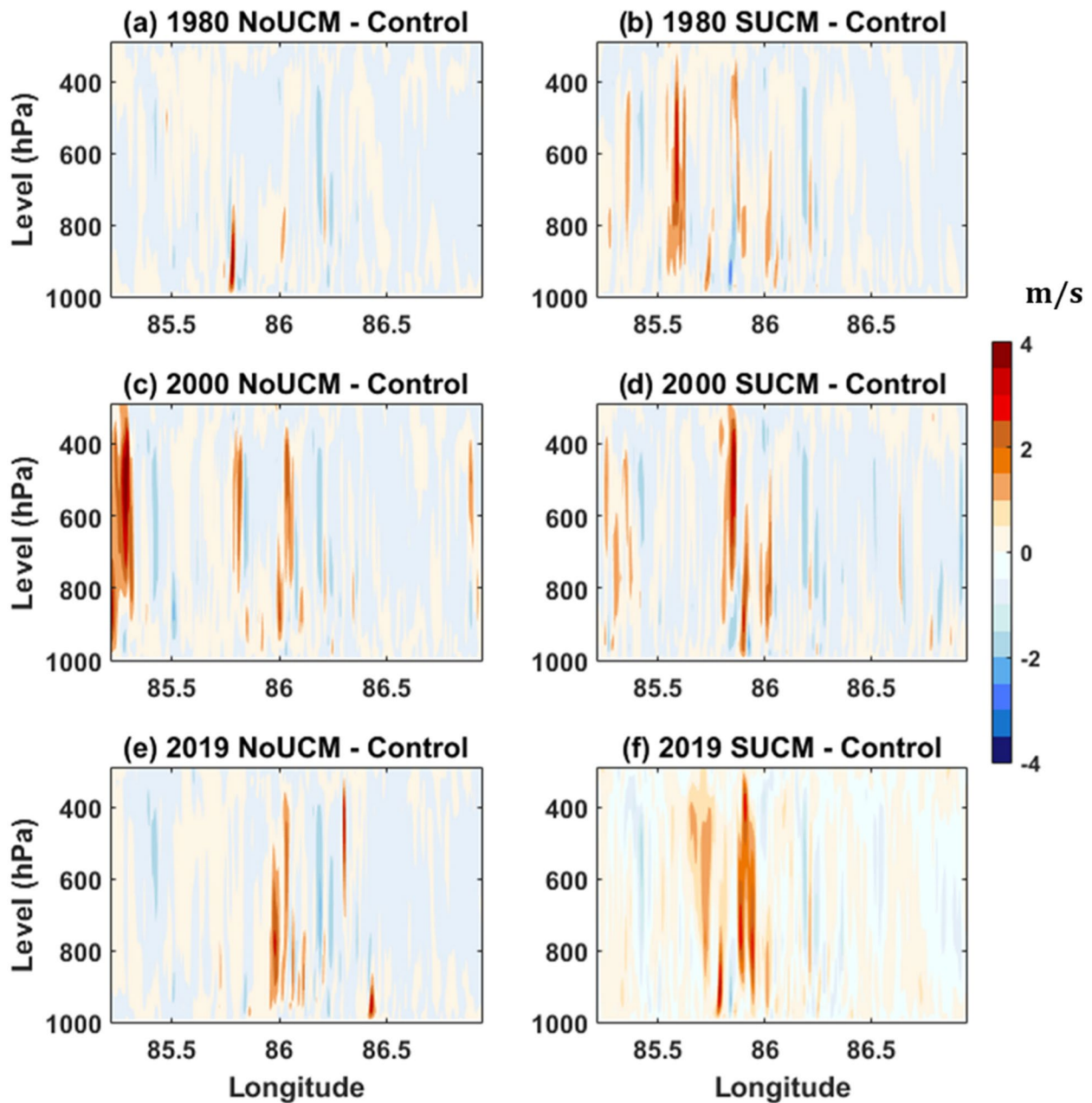
**Fig. 9** Longitude-Level plot for vertical velocity (m s-1) at constant latitude (20.25° N) for 20072018 case **a** 1980 NoUCM– control, **b** 1980 SUCM – control, **c** 2019 NoUCM– control, and **d** 2019 SUCM – control

land state regulates the precipitation efficiency (Schär et al., 1999). Different researchers are also using this method to analyze various processes contributions to precipitation (Osuri et al., 2020). It is suggested that the incorporation of updated LULC in the model provides additional information on understanding the importance of LULC in modulating precipitation, which can be done by surface-precipitation feedback analysis.

The change in precipitation "ΔP" can be expressed as,

$$\triangle P = P^{\backprime} - P = \underbrace{\triangle \chi \, (ET + IN)}_{(I)} + \underbrace{\chi \, (\triangle ET)}_{(II)}$$
$$+ \underbrace{\chi \, \triangle IN}_{(III)} + \underbrace{\triangle \chi (\triangle ET + \triangle IN)}_{(IV)}$$

$$\tag{4}$$

where,

"$\chi$" = precipitation efficiency and calculates as $\chi = \frac{P}{(ET+IN)}$.

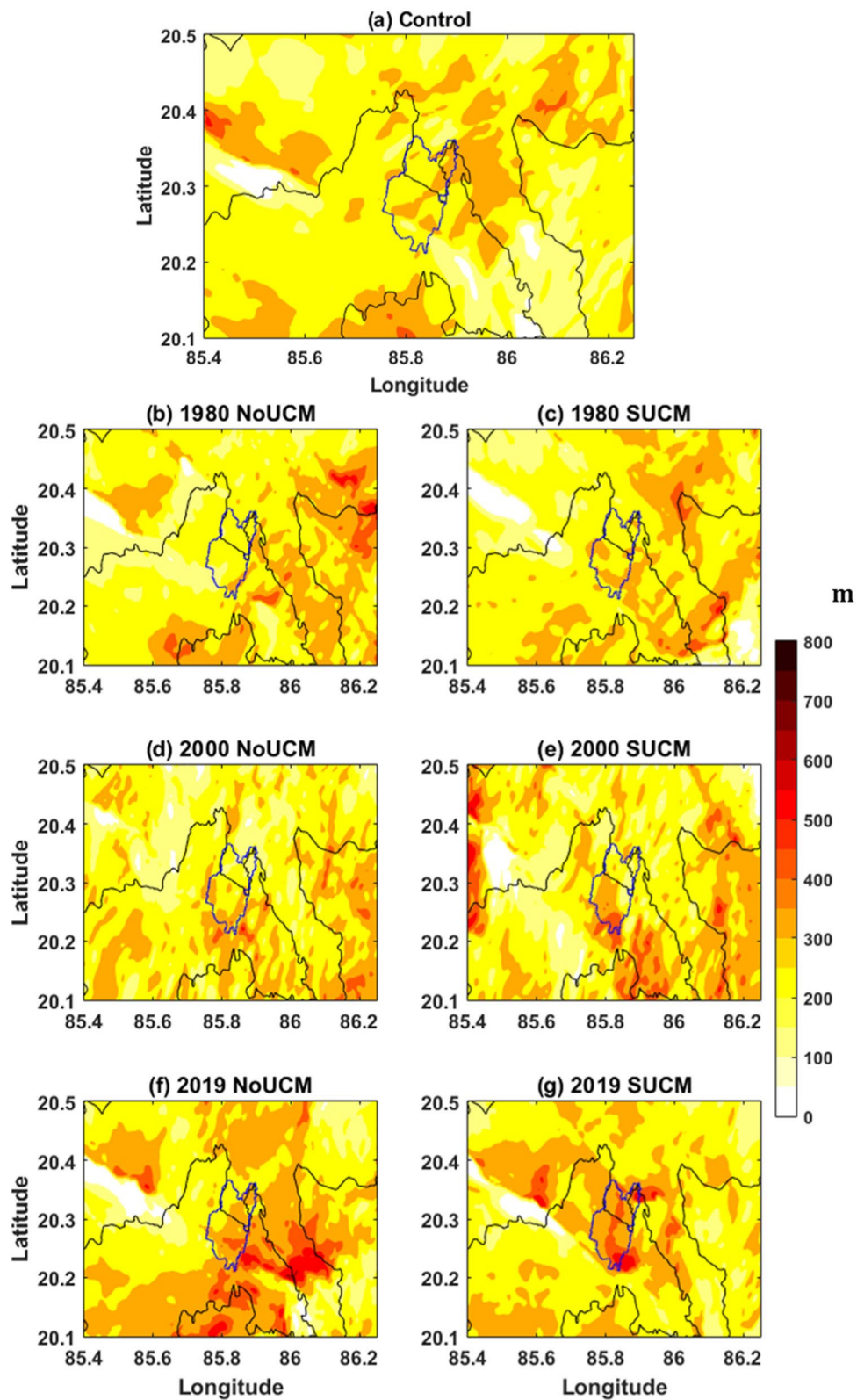"$ET$" = evaporation and "$IN$" = moisture influx.

**Fig. 10** Planetary boundary layer height (m) for 20072018 case **a** control run, **b** 1980 NoUCM, **c** 1980 SUCM, **d** 2000 NoUCM, **e** 2000 SUCM, **f** 2019 NoUCM, and **g** 2019 SUCM

*P'* stands for 1980_NoUCM, 1980_SUCM, 2000_NoUCM, 2000_SUCM, 2019_NoUCM, & 2019_SUCM experiments and *P* stands for control experiment. "Term I" represents the efficiency effect which implies the precipitation change due to precipitation efficiency. "Term II" represents the surface effect which is mainly the evaporation. "Term III" represents remote effect, which represents the impact of remotely present moisture on rainfall, and "Term IV" represents residual term.

$$ET = \frac{Latent\,heat\,flux}{Latent\,heat\,of\,vaporization(\lambda)} \qquad (5)$$

$\lambda = (2.501 - 0.00237 * T_{air})10^6$ (J kg-1), and $T_{air}$ is the air temperature at the ground surface.

The surface-precipitation feedback for the time of heavy rainfall has been averaged over Bhubaneswar (20.2 N – 20.36 N; 85.76E – 85.9E) and plotted for different model simulations in Fig. 11. It is observed that the precipitation difference is more in 2019_SUCM, which suggests that the rainfall from the 2019_SUCM simulation is more compared to other experiments. The surface effect is more prominent in the 2019_SUCM model experiment, followed by the 2000_SUCM, 1980_SUCM and 2019_NoUCM experiments. It is due to an increase in the urban area, which increases surface air temperature and hence evaporation. In 1980_SUCM, the efficiency effect contributes to the precipitation rate. The efficiency and surface effects have a similar role in 2019_SUCM for precipitation. The residual term is in less magnitude for all the experiments.

### 5.7 Errors of rainfall using CRA method
CRA method provides spatial and quantitative errors present in the model-derived rainfall. Previously, this method has been used for rainfall analysis over the Indian Monsoon region (Kumar Das et al., 2014; Sharma et al., 2019 and Osuri et al., 2020). The spatial and quantitative errors of forecasted rainfall concerning GPM data have been analyzed using the CRA method and shown in Fig. 12. CRA has been calculated on the day of heavy rainfall, and it is observed that the 2019_SUCM is predicting a better spatial representation of rainfall than others. There are two features of having more than 64.5 mm (heavy rainfall as per IMD classification). The first one covers more area and has been well predicted from all the model simulations, whereas the second feature is only present in the 2019_SUCM simulation. Error decompositions derived from CRA have been shown in Table 2. For all model simulations, volume error is less than other decomposition errors in the 2019_SUCM experiment, which is about 0.11%. Displacement error is more minor in the 2019_NoUCM simulation followed by 1980_NoUCM, 1980_SUCM, and 2019_SUCM. The model has more pattern errors in predicting rainfall.

## 6 Summary and conclusion
The study investigated the impact of urbanization on spatial–temporal distribution and intensity of rainfall over Bhubaneswar city. Four heavy rainfall events such as 06th March 2017 (72 mm/hr), 23rd May 2018 (55 mm/hr), 20 – 22 July 2018 (220 mm/day), and 04 – 08 August 2018 (390 mm/day) have been considered for LULC
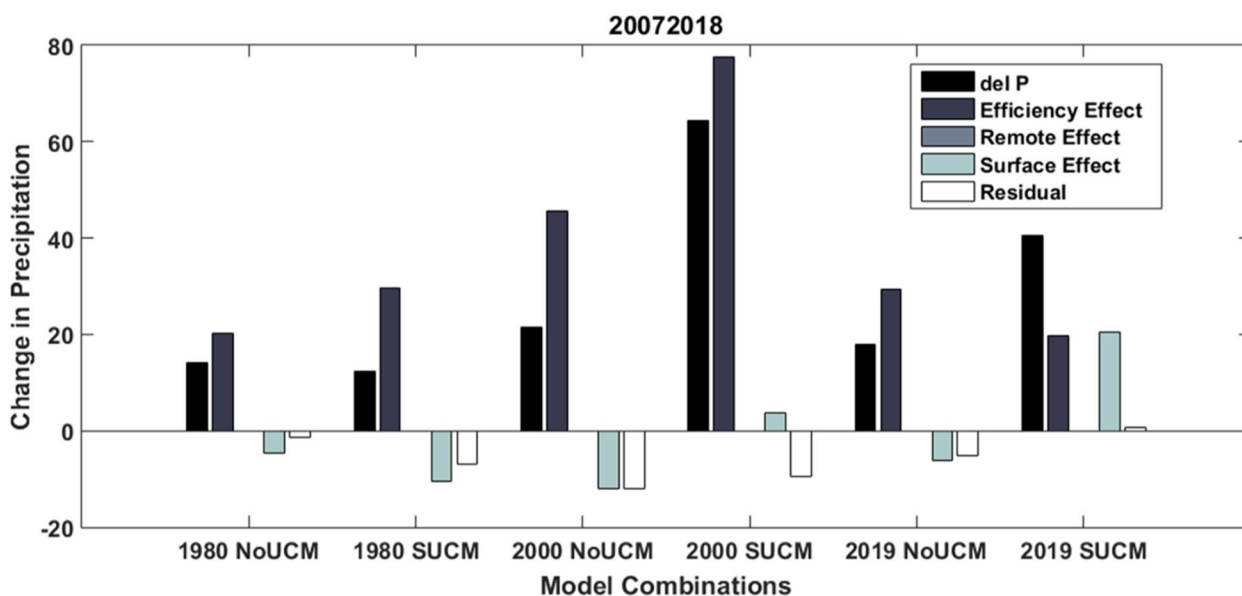


**Fig. 11** Surface-Precipitation Feedback for the heavy rainfall day "x" and "y" level
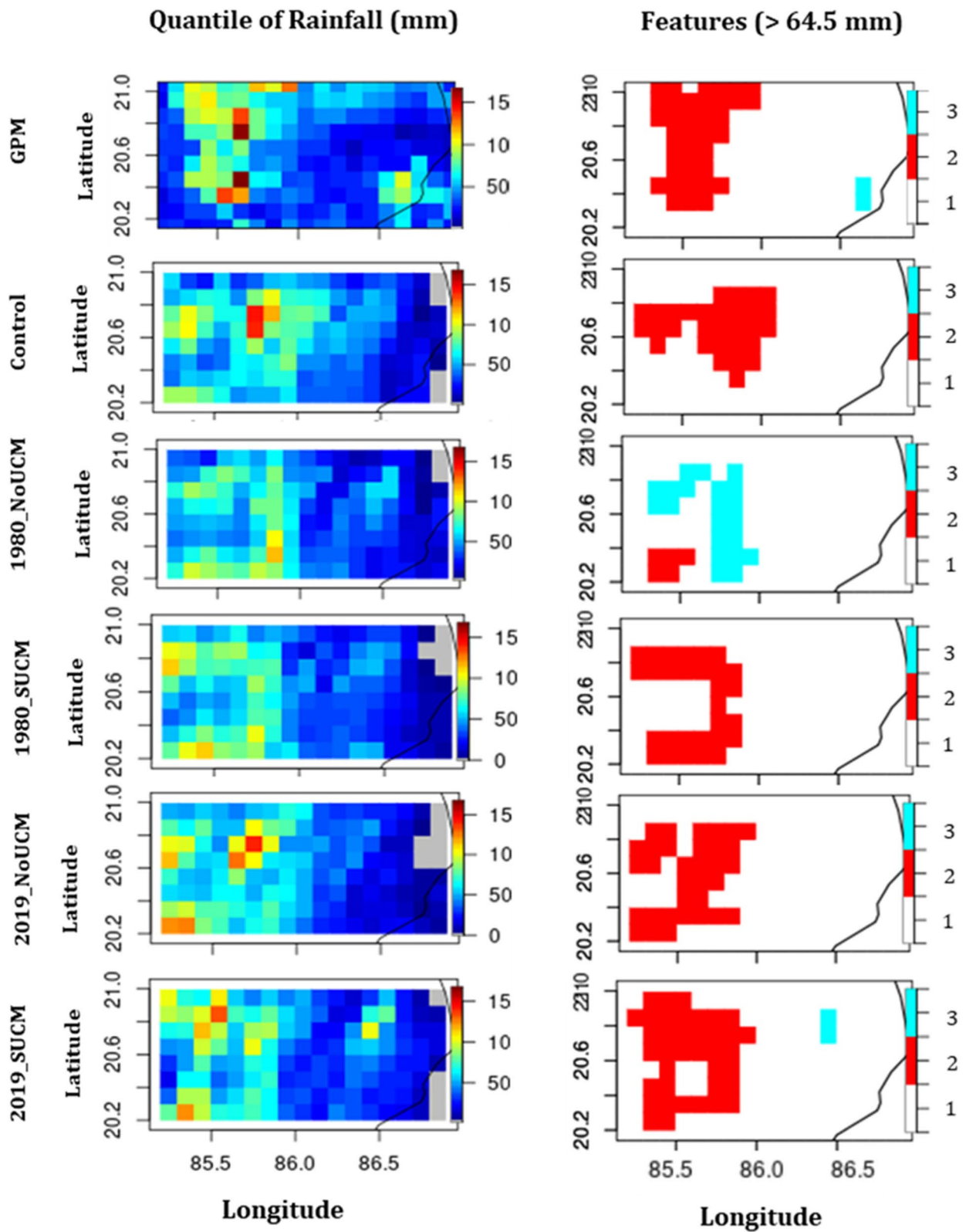
**Fig. 12** Spatial representation of rainfall quantile (first column) and features having rainfall more than 64.5 mm (right column) from observation and model experiments

Swain *et al. Computational Urban Science*    (2023) 3:2

Page 17 of 19

**Table 2** Quantile representation of error decomposition from CRA method

|  | MSE Displacement (%) | MSE Volume (%) | MSE Pattern (%) |
|---|---|---|---|
| Control | 43.49 | 0.24 | 56.27 |
| 1980_NoUCM (Feature 1) | 40.54 | 3.25 | 56.21 |
| 1980_NoUCM (Feature 2) | 19.83 | 16.31 | 63.86 |
| 1980_SUCM | 21.07 | 0.36 | 78.57 |
| 2000_NoUCM | 27.62 | 4.15 | 68.23 |
| 2000_SUCM | 34.13 | 0.28 | 65.59 |
| 2019_NoUCM | 12.77 | 3.31 | 83.92 |
| 2019_SUCM (Feature 1) | 30.26 | 0.11 | 69.63 |
| 2019_SUCM (Feature 2) | 49.22 | 0.45 | 50.33 |

experiments with the help of the WRF mesoscale model. Three different LULC changes, such as 1980, 2000 and 2019, and UCM layer incorporation, have been taken to examine the impact of expansion of urbanized area on rainfall.

The incorporation of LULC in the WRF model reveals that the rainfall intensity has increased in the 2019 LULC simulation in comparison to the 2000 LULC, and 1980 LULC simulations. Model can capture the rainfall in the control experiment but does not accurately predict the spatial distribution of rainfall. Shifting of rainfall occurred in the 2019 LULC with single layer UCM simulation, and more rainfall has happened over the boundary of the urban–rural area. This maximum intensified rainfall only happened for a brief period, i.e., almost one hour, due to the urban heating effect (Dou et al., 2015; Liu & Niyogi, 2019).

Vertically integrated moisture flux is more in the 2019 LULC rainfall simulation, which is over the peripheral region of Bhubaneswar city. Increase in the urban area in 2019 LULC with single layer UCM increases the urban storage flux at the surface. The further positive vertical velocity that suppresses the rising water mass in the atmosphere is present along the city's northern periphery and more in the 2019_SUCM simulation than in the other simulations. PBL height also confirms the impact of urbanization on the local atmosphere and hence on rainfall intensity. Surface-precipitation feedback analysis suggests that the surface effect is more prominent in the 2019_SUCM experiment compared to others. Then, the statistical analysis of model-derived rainfall was carried out, and for this, the object-oriented CRA method was used. From CRA analysis, it is found that the 2019_SUCM simulation accurately captures the spatial and volumetric distribution of heavy rainfall. These outputs are likely to be helpful to urban climate communities for city planning, flooding, and hydro-climatology-related issues.

**References**
Ackerman, B. (1987). Climatology of Chicago area urban-rural differences in humidity. *Journal of Climate and Applied Meteorology,26*(3), 427–430.
Balling, R. C., Jr., & Cerveny, R. S. (1987). Long-term associations between wind speeds and the urban heat island of Phoenix, Arizona. *Journal of Applied Meteorology and Climatology,26*(6), 712–716.
Barik, A., Swain, D., & Vinoj, V. (2019). Rapid urbanization and associated impacts on land surface temperature changes over Bhubaneswar Urban District, India. *Environmental Monitoring and Assessment,191*(3), 790.

Changnon, S. A., Huff, F. A., Schickedanz, P. T., & Vogel, J. L. (1977). Summary of METROMEX, Volume 1: Weather anomalies and impacts. *Illinois State Water Survey Bulletin,62*, 260.

Changnon, S. A., Shealy, R. T., & Scott, R. W. (1991). Precipitation changes in fall, winter, and spring caused by St Louis. *Journal of Applied Meteorology,30*, 126–134.

Chen, T. C., Wang, S. Y., & Yen, M. C. (2007). Enhancement of afternoon thunderstorm activity by urbanization in a valley: Taipei. *Journal of Applied Meteorology and Climatology,46*(9), 1324–1340.

Dou, J., Wang, Y., Bornstein, R., & Miao, S. (2015). Observed spatial characteristics of Beijing urban climate impacts on summer thunderstorms. *Journal of Applied Meteorology and Climatology,54*(1), 94–105.

Ebert, E. E., & Gallus, W. A., Jr. (2009). Toward better understanding of the contiguous rain area (CRA) method for spatial forecast verification. *Weather and Forecasting,24*(5), 1401–1415.

Ebert, E. E., & McBride, J. L. (2000). Verification of precipitation in weather systems: Determination of systematic errors. *Journal of Hydrology,239*(1–4), 179–202.

Ebert, E. E., Wilson, L. J., Brown, B. G., Nurmi, P., Brooks, H. E., Bally, J., & Jaeneke, M. (2004). Verification of nowcasts from the WWRP Sydney 2000 forecast demonstration project. *Weather and Forecasting,19*(1), 73–96.

Ghosh, S., Das, D., Kao, S. C., & Ganguly, A. R. (2012). Lack of uniform trends but increasing spatial variability in observed Indian rainfall extremes. *Nature Clinical Practice Endocrinology & Metabolism,2*(2), 86.

Gogoi, P. P., Vinoj, V., Swain, D., Roberts, G., Dash, J., & Tripathy, S. (2019). Land use and land cover change effect on surface temperature over Eastern India. *Scientific Reports,9*(1), 1–10.

Grams, J. S., Gallus, W. A., Jr., Koch, S. E., Wharton, L. S., Loughe, A., & Ebert, E. E. (2006). The use of a modified Ebert–McBride technique to evaluate mesoscale model QPF as a function of convective system morphology during IHOP 2002. *Weather and Forecasting,21*(3), 288–306.

Gupta, K. (2020). Challenges in developing urban flood resilience in India. *Philosophical Transactions of the Royal Society A,378*(2168), 20190211.

Gupta, A. K., & Nair, S. S. (2010). Flood risk and context of land-uses: Chennai city case. *Journal of Geography and Regional Planning,3*(12), 365–372.

Horton, R. E. (1921). Thunderstorm-breeding spots. *Monthly Weather Review,49*(4), 193–193.

Huff, F. A. (1986). Urban Hydrological Review. *Bulletin of American Meteorological Society,67*, 703–712.

Huff, F. A., & Vogel, J. L. (1978). Urban, topographic and diurnal effects on rainfall in the St, Louis region. *Journal Applied Meteorology,17*, 565–577.

Kishtawal, C. M., Niyogi, D., Tewari, M., Pielke, R. A., Sr., & Shepherd, J. M. (2010). Urbanization signature in the observed heavy rainfall climatology over India. *International Journal of Climatology,30*(13), 1908–1916.

Kumar Das, A., Bhowmick, M., Kundu, P. K., & Roy Bhowmik, S. K. (2014). Verification of WRF rainfall forecasts over India during monsoon 2010: CRA method. *Geofizika,31*(2), 106–126.

Lin, C. Y., Chen, W. C., Liu, S. C., Liou, Y. A., Liu, G. R., & Lin, T. H. (2008). Numerical study of the impact of urbanization on the precipitation over Taiwan. *Atmospheric Environment,42*(13), 2934–2947.

Liu, J., & Niyogi, D. (2019). Meta-analysis of urbanization impact on rainfall modification. *Science and Reports,9*(1), 7301.

Lokoshchenko, M. A. (2017). Urban heat island and urban dry island in Moscow and their centennial changes. *Journal of Applied Meteorology and Climatology,56*(10), 2729–2745.

Moriwaki, R., Watanabe, K., & Morimoto, K. (2013). Urban dry island phenomenon and its impact on cloud base level. *Journal of JSCE,1*(1), 521–529.

Nadimpalli, R., Patel, P., Mohanty, U. C., Attri, S. D., & Niyogi, D. (2022). Impact of urban parameterization and integration of WUDAPT on the severe convection. *Computational Urban Science,2*(1), 1–14.

Niyogi, D., Holt, T., Zhong, S., Pyle, P. C., & Basara, J. (2006). Urban and land surface effects on the 30 July 2003 mesoscale convective system event observed in the southern Great Plains. *Journal of Geophysical Research,111*, D19107. https://doi.org/10.1029/2005JD006746

Niyogi, D., Pyle, P., Lei, M., Arya, S. P., Kishtawal, C. M., Shepherd, M., & Wolfe, B. (2011). Urban modification of thunderstorms: An observational storm climatology and model case study for the Indianapolis urban region. *Journal of Applied Meteorology and Climatology,50*(5), 1129–1144.

Niyogi, D., Osuri, K. K., Busireddy, N. K. R., & Nadimpalli, R. (2020). Timing of rainfall occurrence altered by urban sprawl. *Urban Climate,33*, 100643.

Oke, T. R. (1988). The urban energy balance. *Progress in Physical Geography,12*(4), 471–508.

Osuri, K. K., Nadimpalli, R., Mohanty, U. C., Chen, F., Rajeevan, M., & Niyogi, D. (2017). Improved prediction of severe thunderstorms over the Indian Monsoon region using high-resolution soil moisture and temperature initialization. *Science Reports,7*, 41377.

Osuri, K. K., Nadimpalli, R., Ankur, K., Nayak, H. P., Mohanty, U. C., Das, A. K., & Niyogi, D. (2020). Improved Simulation of Monsoon Depressions and Heavy Rains From Direct and Indirect Initialization of Soil Moisture Over India. *Journal of Geophysical Research: Atmospheres,125*(14), e2020JD032400.

Panda, D. K., Mishra, A., Kumar, A., Mandal, K. G., Thakur, A. K., & Srivastava, R. C. (2014). Spatiotemporal patterns in the mean and extreme temperature indices of India, 1971–2005. *International Journal of Climatology,34*(13), 3585–3603.

Pathy, A. C., & Panda, G. K. (2012). Modeling urban growth in Indian situation-a case study of Bhubaneswar city. *International Journal of Scientific and Engineering Research,3*(6), 1–7.

Pattanaik, D. R., Mukhopadhyay, B., & Kumar, A. (2012). Monthly Forecast of Indian Southwest Monsoon Rainfall Based on NCEP's Coupled Forecast System. *Atmosphere and climate sciences,2*, 479–491.

Pearlmutter, D., Berliner, P., & Shaviv, E. (2005). Evaluation of urban surface energy fluxes using an open-air scale model. *Journal of Applied Meteorology,44*(4), 532–545.

Pielke, R. A., Pitman, A., Niyogi, D., Mahmood, R., McAlpine, C., Hossain, F., Goldewijk, K. K., Nair, U., Betts, R., Fall, S., & Reichstein, M. (2011). Land use/land cover changes and climate: Modeling analysis and observational evidence. *Wiley Interdisciplinary Reviews: Climate Change,2*(6), 828–850.

Rozoff, C. M., Cotton, W. R., & Adegoke, J. O. (2003). Simulation of St. Louis, Missouri, land use impacts on thunderstorms. *Journal of Applied Meteorology,42*, 716–738.

Schär, C., Lüthi, D., Beyerle, U., & Heise, E. (1999). The soil–precipitation feedback: A process study with a regional climate model. *Journal of Climate,12*(3), 722–741.

Sharma, K., Ashrit, R., Ebert, E., Mitra, A., Bhatla, R., Iyengar, G., & Rajagopal, E. N. (2019). Assessment of Met Office Unified Model (UM) quantitative precipitation forecasts during the Indian summer monsoon: Contiguous Rain Area (CRA) approach. *Journal of Earth System Science,128*(1), 1–17.

Shepherd, J. M. (2005). A review of current investigations of urban-induced rainfall and recommendations for the future. *Earth Interactions,9*(12), 1–27.

Shepherd, J. M., Pierce, H., & Negri, A. J. (2002). Rainfall modification by major urban areas: Observations from spaceborne rain radar on the TRMM satellite. *Journal of Applied Meteorology,41*(7), 689–701.

Swain, D., Roberts, G. J., Dash, J., Lekshmi, K., Vinoj, V., & Tripathy, S. (2017). Impact of rapid Urbanization on the city of Bhubaneswar, India. *Proceedings of the National Academy of Sciences, India Section a: Physical Sciences,87*(4), 845–853.

Van Zomeren, J., & Van Delden, A. (2007). Vertically integrated moisture flux convergence as a predictor of thunderstorms. *Atmospheric Research,83*(2–4), 435–445.

Yan, Z. W., Wang, J., Xia, J. J., & Feng, J. M. (2016). Review of recent studies of the climatic effects of urbanization in China. *Advances in Climate Change Research,7*(3), 154–168.

Zhang, S., Huang, G., Qi, Y., & Jia, G. (2018). Impact of urbanization on summer rainfall in Beijing–Tianjin–Hebei metropolis under different climate backgrounds. *Theoretical and Applied Climatology,133*(3–4), 1093–1106.

Zhang, H., Wu, C., Chen, W., & Huang, G. (2019). Effect of urban expansion on summer rainfall in the Pearl River Delta, South China. *Journal of Hydrology,568*, 747–757.

Zhong, S., & Yang, X. (2015). Ensemble simulations of the urban effect on a summer rainfall event in the great Beijing metropolitan area. *Atmospheric Research,153*, 318–334.

Banacos, P. C., & Schultz, D. M. (2005). The use of moisture flux convergence in forecasting convective initiation: Historical and operational perspectives. *Weather and Forecasting, 20*(3), 351–366.

Mohanty, U. C., Mohapatra, M., Singh, O. P., Bandyopadhyay, B. K., & Rathore, L. S. (Eds.). (2013). Monitoring and prediction of tropical cyclones in the Indian Ocean and climate change. *Springer Science & Business Media.*

Niyogi, D., Subramanian, S., Mohanty, U.C., Kishtawal, C.M., Ghosh, S., Nair, U.S., Ek, M., Rajeevan M. (2018). *The impact of land cover and land use change on the Indian monsoon region hydroclimate*. Land-Atmospheric Research Applications in South and Southeast Asia, Springer, Cham, pp. 553–575

Shepherd, J. M. (2013). Impacts of urbanization on precipitation and storms: Physical insights and vulnerabilities. In *Climate Vulnerability (Vol. 5, pp. 109– 125)*. Elsevier.

Skamarock, W. C., Klemp, J. B., Dudhia, J., Gill, D. O., Barker, D. M., Wang, W., & Powers, J. G. (2005). A description of the advanced research WRF version 2 (No. NCAR/TN-468+ STR). National Center For Atmospheric Research Boulder Co Mesoscale and Microscale Meteorology Div.

Swain M, Nadimpalli R, Mohanty U C and Pattnaik S.; Impact of cumulus convection in predicting heavy rainfall events over Odisha: sensitivity to cloud micro-physics; International Workshop on Modeling Atmospheric - Oceanic Processes for Weather and Climate Extremes (MAPEX 2019); March 28–29, 2019; IIT Delhi.

## Publisher's Note